Lawrence Berkeley National Laboratory
Recent Work

Title

KINETICS OF COARSENING

Permalink

https://escholarship.org/uc/item/2qf811k9

Authors

Nunes, A.C.
Wallace, J.M.
Dorn, J.E.

Publication Date

1965-08-01

University of California

Ernest O. Lawrence Radiation Laboratory

KINETICS OF COARSENING

Berkeley, California

DISCLAIMER

UNIVERSITY OF CALIFORNIA

Lawrence Radiation Laboratory
Berkeley, California

AEC Contract No. W-7405-eng-48

KINETICS OF COARSENING

A. C. Nunes, Jr.,[1] J. M. Wallace[2] and J. E. Dorn[3]

August, 1965

[1] Research Assistant, Inorganic Materials Research Division of the Lawrence Radiation Laboratory, University of California, Berkeley.

[2] Research Assistant, Inorganic Materials Research Division of the Lawrence Radiation Laboratory, University of California, Berkeley.

[3] Professor of Materials Science of the Department of Mineral Technology and Research Metallurgist of the Inorganic Materials Research Division of the Lawrence Radiation Laboratory, University of California, Berkeley.

INTRODUCTION

When an alloy consisting of a dispersed phase in an alpha solid solution matrix is annealed, the larger particles grow and the finer particles decrease in size until they finally dissolve. Such coarsening reactions are important in a number of practical problems. Current knowledge on the theory of coarsening has recently been discussed by Fine[1] in terms of analyses previously presented by Greenwood[2] and by Lifschitz and Slezov.[3] It is the purpose of this report to provide a simple solution to the problem and to formulate the method of analysis so as to facilitate the application of the theory to experimental data.

ANALYSIS

Particles of the precipitated phase will be assumed to be uniformly dispersed throughout the matrix as spheres having a distribution of radii, α. At the surface of each particle the concentration of the solute in the matrix will be taken to be the equilibrium value[2]

$$C_\alpha = C_o e^{\frac{2\Omega\gamma}{\alpha kT}} \simeq C_o(1 + \frac{2\Omega\gamma}{\alpha kT}) \tag{1}$$

where C_o is the concentration of the solute in the matrix at a flat particle surface, Ω is the volume per solute atom in the precipitate phase, γ is the unit free surface energy, and kT has its usual significance of the Boltzmann constant times the absolute temperature. The approximation of Eq. (1) is quite accurate since $\frac{2\Omega\gamma}{\alpha kT} \ll 1$ for interesting values of kT even when α has its smallest value at a, e. g. about 2 atomic diameters. Therefore the average solute concentration in the matrix is

$$\overline{C} = C_o (1 + \frac{2\Omega\gamma}{kT} \frac{1}{\hat{a}}) \tag{2}$$

where $\frac{1}{\hat{a}} = (\overline{\frac{1}{\alpha}})$, namely the average value of the reciprocal of the radii. As a consequence of their random distribution each particle can be thought to be surrounded by a sphere of influence of radius R such that

$$N = \frac{1}{\frac{4\pi}{3}R^3} \tag{3}$$

where N is the total number of particles per unit volume. Whereas $C = C_\alpha$ at the surface of a particle of radius $r = \alpha$, on the average $C = \overline{C}$ at $r = R$. Those particles for which $C_\alpha > \overline{C}$ will dissolve and those for which $C_\alpha < \overline{C}$ will increase in size. Assuming steady state

spherical diffusion for this process, the concentration C as a function

of r about every particle is given by[3]

$$C = \frac{K_1}{r} + K_2 \qquad (4)$$

where, upon introducing the previously quoted boundary conditions,

$$K_1 = \frac{2C_o \Omega \gamma R \alpha}{kT(R-\alpha)} \left\{ \frac{1}{\alpha} - \frac{1}{\hat{\alpha}} \right\} \qquad (5)$$

and K_2 is a constant. Consequently the concentration gradient at the

surface of a particle is

$$\left(\frac{\partial C}{\partial r} \right)_{r=\alpha} = - \frac{K_1}{\alpha^2} = \frac{2C_o \Omega \gamma}{kT} \frac{R}{\alpha(R-\alpha)} \left\{ \frac{1}{\hat{\alpha}} - \frac{1}{\alpha} \right\} \qquad (6)$$

and therefore the total diffusional flux away from a particle of radius

α is

$$- 4\pi\alpha^2 M \frac{d\alpha}{dt} = 4\pi\alpha^2 D \left(-\frac{\partial C}{\partial r} \right)_{r=\alpha} = - 4\pi\alpha^2 D \left(\frac{2C_o \Omega \gamma}{kT} \right) \frac{R}{\alpha(R-\alpha)} \left\{ \frac{1}{\hat{\alpha}} - \frac{1}{\alpha} \right\} \qquad (7)$$

where M is the moles solute per unit volume of the particle and D

is the diffusivity of solute in the matrix. Equation (7) may be placed

in dimensionless form by letting

$$x = \frac{\alpha}{\hat{\alpha}} \qquad (8a)$$

and

$$t = \frac{MkT}{2C_o \Omega \gamma D \hat{\alpha}_o^3} \int_0^\theta \frac{d\theta}{(\hat{\alpha}/\hat{\alpha}_o)^3} \qquad (8b)$$

where x is a normalized radius of a particle and θ is the proper time

variable. On this basis

$$\frac{x^2(1-\frac{\hat{\alpha}}{R}x)dx}{(1-x)} = - d\theta \qquad (9)$$

Although $\frac{\hat{\alpha}}{R}$ depends on θ, its variation with θ can be taken to remain substantially constant for not too large changes in θ. Furthermore $\frac{\hat{\alpha}}{R} x$ is often small relative to unity and in this case it has only a minor effect on the solution.

For the condition of constant $\frac{\hat{\alpha}}{R}$ Eq. (9) can be integrated to give

$$\theta = \frac{x^2-x_o^2}{2} + x - x_o + \ln\left|\frac{x-1}{x_o-1}\right| + \frac{\hat{\alpha}}{R}\left[\frac{x_o^3-x^3}{3} + \frac{x_o^2-x^2}{2} + x_o - x - \ln\left|\frac{x-1}{x_o-1}\right|\right]$$

$$(10)$$

where x and x_o are the normalized particle radii at the proper times θ and $\theta = 0$ respectively.

The variation of the normalized particle radii x with the proper time θ is shown in Fig. 1 for the case $\frac{\hat{\alpha}}{R} \ll 1$. These are universal curves that are independent of the distribution of particle sizes. As the proper time θ increases the smaller particles rapidly decrease in size while the larger particles get only slightly larger. Those particles for which $x = \frac{\alpha}{\hat{\alpha}} = 1$ remain unchanged in size. It is necessary, however, to bear in mind that $\hat{\alpha}$ itself changes with θ dependent upon the distribution of particle sizes α.

Since the natural variable for the integration of Eq. (9) was found to be the normalized radius $x = \frac{\alpha}{\hat{\alpha}}$, it is convenient also to describe any distribution of particle sizes in terms of this same variable. Accordingly the number of particles per unit volume dN_o initially having relative radii between x_o and $x_o + dx_o$ will be given by $dN_o = \phi_o\{x_o\} dx_o$. Thus

$$N_o = \int_o^\infty \phi\,\{x_o\}\,dx_o \qquad (11)$$

As shown by Fig. 1 the smaller particles ever more rapidly decrease in size as θ increases and finally dissolve. Although such dissolution occurs when $x = \frac{a}{\hat{a}}$ where a might be, for example, about twice the atomic radius of the precipitate species, to an extremely high degree of accuracy such dissolution can effectively be taken to occur when $x = 0$. Thus, as shown by Eq. (10), all particles of initial relative sizes less than x_o' will have dissolved at the proper time θ where as shown in Fig. 2

$$\theta = -\frac{x_o'^2}{2} - x_o' + \ln\left|\frac{-1}{x_o'-1}\right| + \frac{\hat{a}}{R}\left[\frac{x_o'^3}{3} + \frac{x_o'^2}{2} + x_o' - \ln\left|\frac{-1}{x_o'-1}\right|\right] \quad (12)$$

but all other particles still exist, albeit with new adjusted radii. Thus the number of particles N at any appropriate time θ is

$$N = \int_{x_o'\{\theta\}}^\infty \phi\{x_o\}\,dx_o \qquad (13)$$

To complete the solution of this problem it is merely necessary to establish the real time t as a function of θ. Such a relationship follows from the conservation of mass namely

$$Mv_p + \overline{C}\,(1 - v_p) = \text{constant} \qquad (14)$$

where v_p is the precipitate phase volume per unit total volume, i. e.

$$v_p = \frac{4\pi}{3}\int_{x_o'\{\theta\}}^\infty a^3\,\phi\{x_o\}dx_o = \frac{4\pi}{3}\hat{a}^3\int_{x_o'\{\theta\}}^\infty x^3\,\phi\{x_o\}dx_o \qquad (15)$$

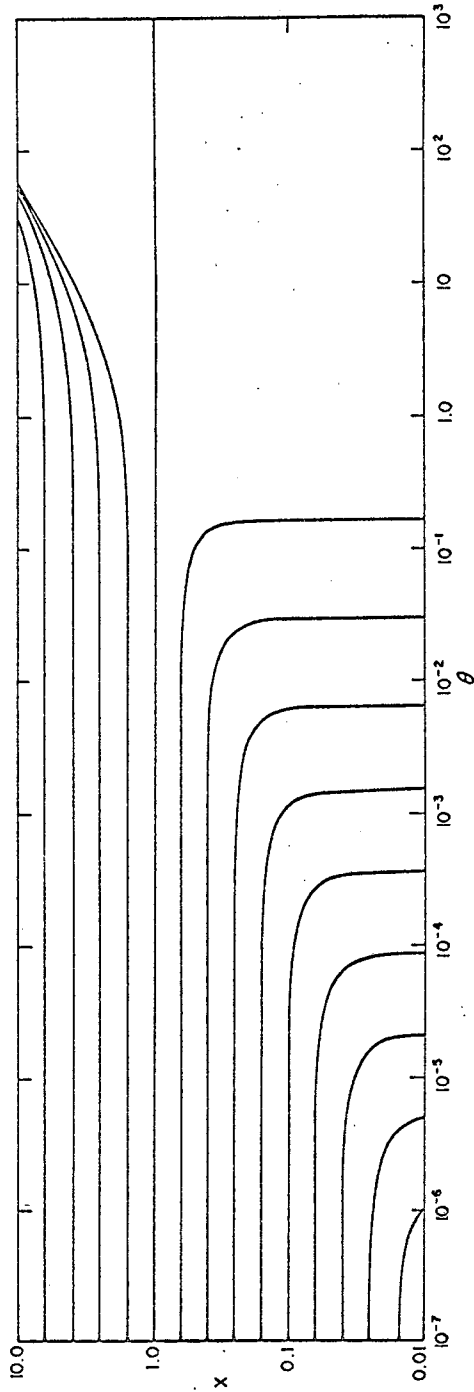Rearranging Eq. (14), inserting Eq. (2), and assuming v_p and $\frac{\overline{C}}{M}$ much smaller than unity

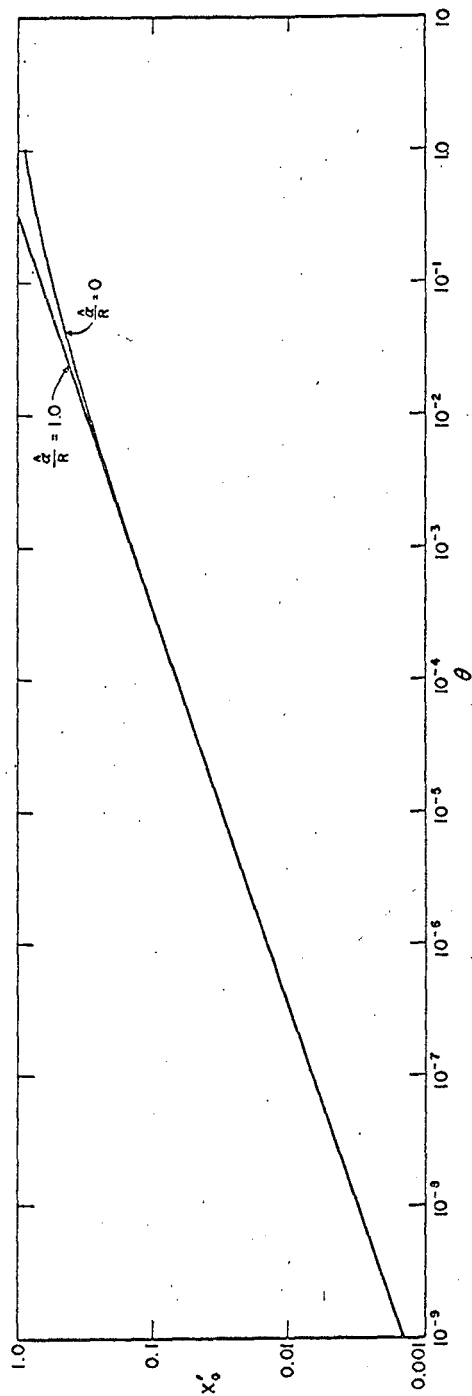FIG I. PARTICLE SIZE TRAJECTORIES FOR $\frac{a}{R} = 0.$

MUB-7430

Fig. 1

FIG. 2 INITIAL PARTICLE SIZE vs. PROPER DISAPPEARANCE TIME.

Fig. 2

MUB-7429

$$v_p \simeq v_{po} + \left(\frac{2\Omega\gamma C_o}{\hat{\alpha}_o kTM}\right)\left(\frac{\hat{\alpha}-\hat{\alpha}_o}{\hat{\alpha}}\right) \tag{16}$$

where v_{po} and $\hat{\alpha}_o$ are the initial phase volume and mean particle radius respectively. Equations (15) and (16) can be used to determine $\hat{\alpha}$ for new particle distributions for most cases one would expect to encounter.

To obtain the real time Eq. (8b) is integrated using the value of $\hat{\alpha}^3$ as obtained from Eqs. (15) and (16). Whereas the changes of the relative radii x with 6 are independent of the distribution of the dispersion, the variation of N, R, and $\hat{\alpha}$ with t depend on the distribution. In general, therefore, the rate of coarsening is dependent on the initial distribution and is not a unique function of the time, t.

DISCUSSION

The various implications of the theory of coarsening are best described in terms of an hypothetical example. For this purpose a uniform initial distribution of particle sizes will be assumed such that

$$dN_o = \psi\{\alpha_o\}d\alpha_o = \overline{K} \, d\alpha_o = \phi\{x_o\}dx_o \qquad (17)$$

where $\overline{K} = \begin{cases} 0 \text{ for } 0 \le \alpha_o < \alpha_{o-} \\ \text{constant for } \alpha_{o-} \le \alpha_o \le \alpha_{o+} \\ 0 \text{ for } \alpha_{o+} < \alpha_o < \infty \end{cases}$

Thus

$$N_o = \overline{K} \, (\alpha_{o+} - \alpha_{o-}) \qquad (18a)$$

$$\frac{1}{\hat{\alpha}_o} = \frac{1}{N_o}\int_{\alpha_{o-}}^{\alpha_{o+}} \frac{\overline{K}d\alpha_o}{\alpha_o} = \frac{1}{\alpha_{o+}-\alpha_{o-}} \ln \frac{\alpha_{o+}}{\alpha_{o-}} \qquad (18b)$$

$$\phi\{x_o\} = \overline{K} \, \hat{\alpha}_o = \frac{N_o}{\ln\dfrac{\alpha_{o+}}{\alpha_{o-}}} \qquad (18c)$$

A few numbers assist in visualizing the issues. Let, for example, $N_o = 10^8$ cm^{-3}, $\alpha_{o+} = 10^{-3}$ cm, and $\alpha_{o-} = 10^{-5}$ cm. Then $\overline{K} \equiv 1.01 \times 10^{11}$cm^{-2} and $\hat{\alpha}_o \equiv 2.15 \times 10^{-4}$ cm. Thus whereas $\overline{K}$ is determined primarily by the larger sized particles, the important quantity $\hat{\alpha}_o$ is weighted by the smaller sized particles. In fact $\hat{\alpha}_o$ is usually less than the resolution of the optical microscope, which illustrates that the previously employed optical methods for studying coarsening of dispersions are

wholly inadequate. However, electron microscopy, coupled with optical

microscopy when needed, could provide the requisite data.

The distribution function of Eq. (17) is shown on the left side

of Fig. 3. In this example

$$\frac{\hat{\alpha}_o}{R} = \hat{\alpha}_o \left(\frac{4\pi}{3} N_o \right)^{1/3} = 0.161$$

which does not permit neglecting $\frac{\hat{\alpha}}{R}$.

Taking short enough time intervals for $\frac{\hat{\alpha}}{R}$ to be effectively constant

over the interval new particle sizes may be successively calculated

from Eq. (10) and also new $\hat{\alpha}$'s from Eqs. (15) and (16) with the

arbitrary but plausible, with respect to magnitude, assumption that

$\frac{\Omega \gamma C_o}{\hat{\alpha}_o MkT} = 0.97 \times 10^{-11}$. This was done by machine to obtain the particle

trajectories shown in Fig. 3. To the left of the figure is shown the

distribution of particle sizes for over 4 orders of magnitude increase

in proper time after the first particle dissolves at about $\theta = 3.5 \times 10^{-5}$

to when about 25% of the particles have dissolved. The distribution

was calculated by noting that the number of particles between trajectory

lines must be constant; hence

$$(x_2 - x_1) \, \phi_{12} = (x_{o2} - x_{o1}) \, \phi_{o12} \tag{19}$$

where 1 and 2 are subscripts referring to a particular trajectory line

and ϕ_{12} is the average distribution density between the lines. Thus

when the lines open up the distribution density of particles decreases

and conversely; the reader should take care, however, not to be

deceived by the logarithmic nature of the graphs actually presented in

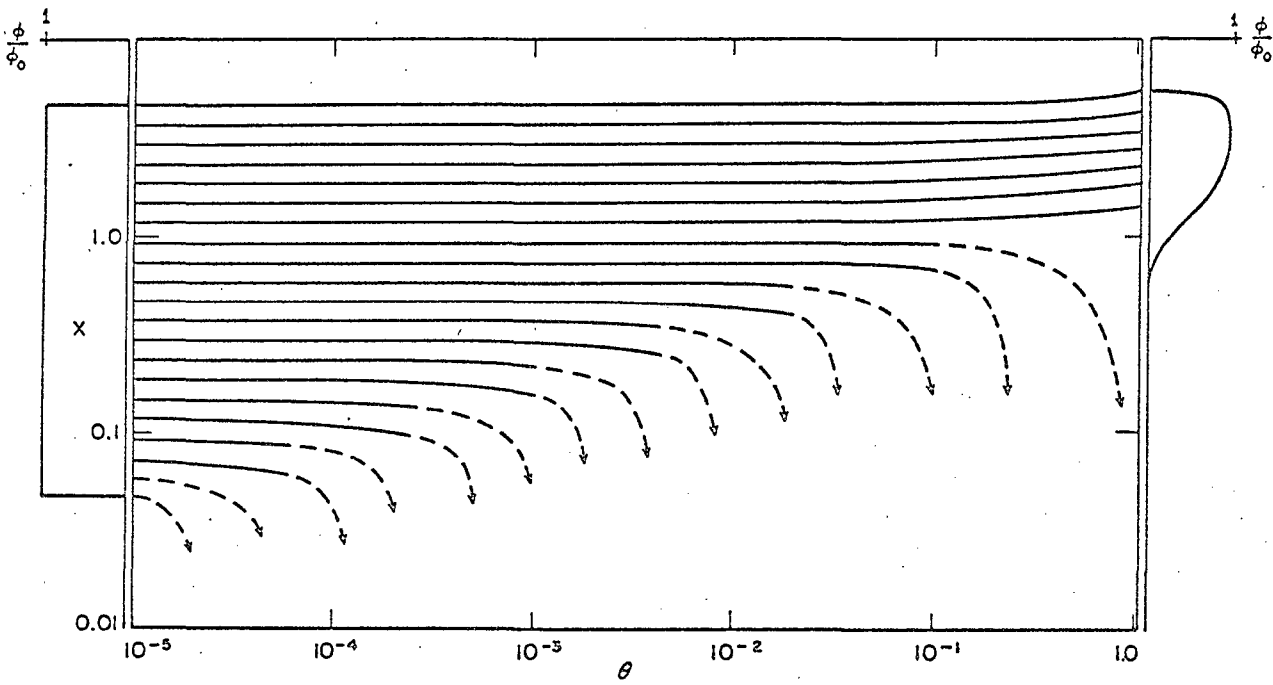Figs. 1 and 3 where lines appearing to go together may actually be

FIG.3 PARTICLE SIZE TRAJECTORIES FOR SAMPLE PROBLEM.

MUB-7428

Fig. 3

diverging on an undistorted plot.

As shown in Fig. 4, the actual time and the proper time used for convenience in solving the problem differ very little and $\hat{a}$ changes only slightly; a plot of a trajectories vs. actual time would look so much like Fig. 3 that there would be no detectable difference save for a shift downwards, the small decrease in $\hat{a}$ is a characteristic of the distribution selected; shrinkage of particles in this case decreases $\hat{a}$ faster than the disappearance of small particles increases it. Ultimately as the small particles are consumed to leave only large ones $\hat{a}$ must increase.

Knowledge of the radius distribution enables the calculation of any quantity dependent on this distribution -such as the spacing between particles also shown in Fig. 4. The variation of $\frac{\hat{a}}{R}$ is due largely to the variation of particle spacing and can be seen to decrease by around 10% by the time about 25% of the particles have disappeared.

A complete quantitative analysis of coarsening as illustrated above requires detailed knowledge of the distribution of particles and other data that are not usually available. On the other hand the general trends suggested by the theory can be applied qualitatively to provide judgment regarding solution of many practical problems. Only one will be described here: Most creep resistant alloys are precipitation hardened. The present discussion is not to be directed toward those cases where the strengthening results primarily from coherency stresses but will refer rather to the pertinent example of finely dispersed incoherent phases in a matrix. As coarsening takes
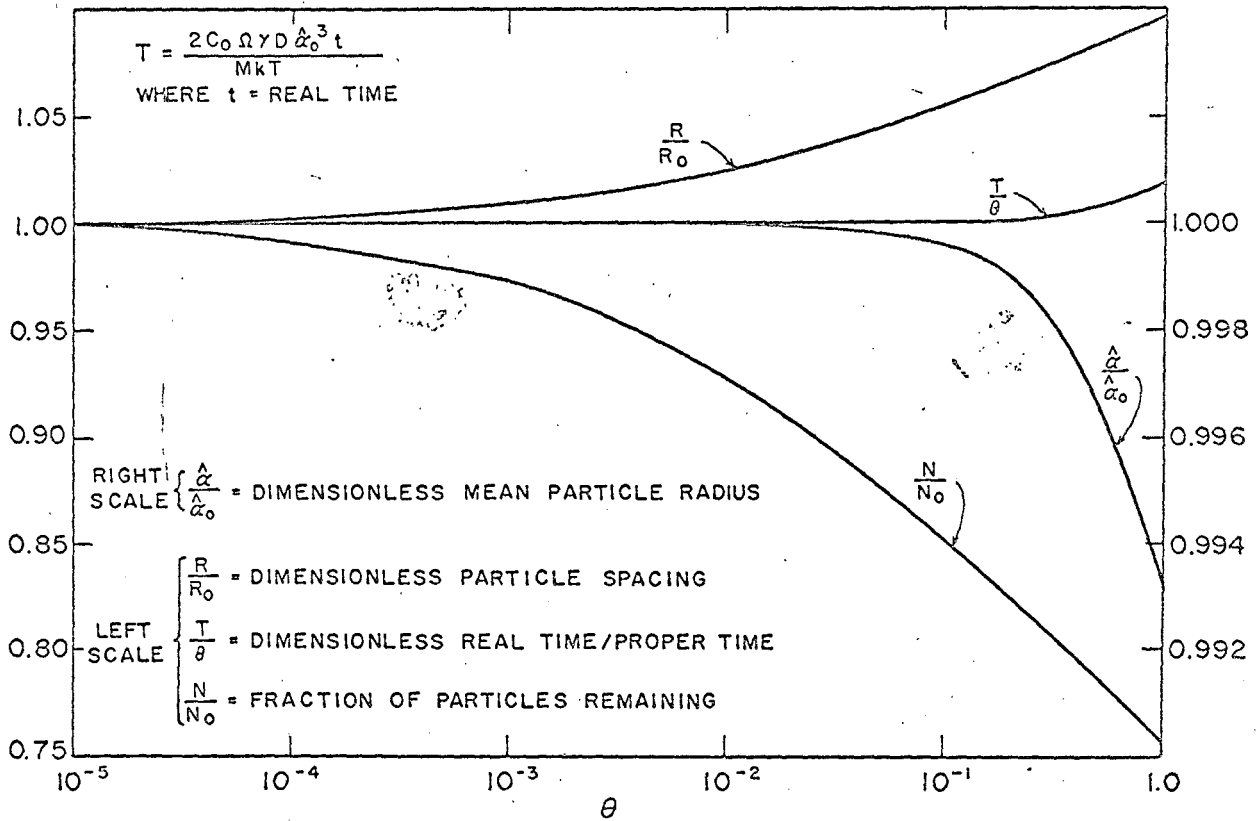
FIG. 4 SELECTED PARAMETERS OF SAMPLE PROBLEM vs. PROPER TIME.

MUB-7427

Fig. 4

place the creep resistance decreases. Consequently the most coarsening
resistant dispersion is best for long term creep resistance. The key
for selection of the most stable dispersion is contained in Eq. (8b),
where it can be noted that the most desirable condition is obtained by
the largest values of $\frac{C_o \Omega \gamma D}{MkT}$ and the smallest values of $\mathcal{a}^3$. Usually
very little control can be exercised over $\mathcal{a}^3$ because small values of $\mathcal{a}^3$
are needed to achieve the desired strengthening. On the other hand if
a material could be so compounded, by mixing powders, as suggested
by the previously described distribution, that no very small particles
were initially present, no dissolution of particles would take place
for some time. The major issue in preparing a stable dispersion, however,
is satisfied when $\frac{C_o \Omega \gamma D}{MkT}$ is as large as possible. Although large surface
energies are desireable there is little opportunity to improve the stability of
a dispersion strengthened alloy from this approach. Thus it appears
that for two precipitates having about the same surface energy the coefficient
of merit for stability, M, can be expressed by

$$\frac{M_1}{M_2} = \frac{C_{o2} D_2}{C_{o1} D_1}$$

and by far the most control can be exercised by selecting the precipitate
such that C_o is as small as possible. Such precipitates have the
lowest free energies of formation.

The rather sharp upper temperature limit for creep resistance of
a dispersion strenghened alloy is a direct result of the rapid increase
of both C_o and D with increasing temperatures.

ACKNOWLEDGMENTS

REFERENCES

1. M. E. Fine, <u>Phase Transformations in Condensed Systems</u>, Macmillan (1964).

2. G. W. Greenwood, Acta Met., $\underline{4}$, 243 (1956).

3. I. M. Lifschitz and V. V. Slezov, Soviet Physics J.E.T.P., $\underline{35}$ (8) No. 2 (1959).